Molecular Plant Pathology

MOLECULAR PLANT PATHOLOGY (2018) 19(8), 1995–2010 DOI: 10.1111/mpp.12675

Isochorismate-based salicylic acid biosynthesis confers basal resistance to *Fusarium graminearum* in barley

QUNQUN HAO[1,2,3,†], WENQIANG WANG[1,4,†], XIULI HAN[1,2‡], JINGZHENG WU[1,2], BO LYU[3], FENGJUAN CHEN[1], ALLAN CAPLAN[3], CAIXIA LI[1,2], JIAJIE WU[1,2], WEI WANG[1,4], QIAN XU[1,2,*] AND DAOLIN FU[3,5,*]

[1]*State Key Laboratory of Crop Biology, Shandong Agricultural University, Taian, Shandong 271018, China*
[2]*College of Agronomy, Shandong Agricultural University, Taian, Shandong 271018, China*
[3]*Department of Plant Sciences, University of Idaho, Moscow, ID 83844, USA*
[4]*College of Life Sciences, Shandong Agricultural University, Taian, Shandong 271018, China*
[5]*Center for Reproductive Biology, Washington State University, Pullman, WA 99164, USA*

SUMMARY

Salicylic acid (SA) plays an important role in signal transduction and disease resistance. In *Arabidopsis*, SA can be made by either of two biosynthetic branches, one involving isochorismate synthase (ICS) and the other involving phenylalanine ammonia-lyase (PAL). However, the biosynthetic pathway and the importance of SA remain largely unknown in Triticeae. Here, we cloned one *ICS* and seven *PAL* genes from barley, and studied their functions by their overexpression and suppression in that plant. Suppression of the *ICS* gene significantly delayed plant growth, whereas *PAL* genes, both overexpressed and suppressed, had no significant effect on plant growth. Similarly, suppression of *ICS* compromised plant resistance to *Fusarium graminearum*, whereas similar suppression of *PAL* genes had no significant effect. We then focused on transgenic plants with *ICS*. In a leaf-based test with *F. graminearum*, transgenic plants with an up-regulated *ICS* were comparable with wild-type control plants. By contrast, transgenic plants with a suppressed *ICS* lost the ability to accumulate SA during pathogen infection and were also more susceptible to *Fusarium* than the wild-type controls. This suggests that ICS plays a unique role in SA biosynthesis in barley, which, in turn, confers a basal resistance to *F. graminearum* by modulating the accumulation of H_2O_2, O_2^- and reactive oxygen-associated enzymatic activities. Although SA mediates systemic acquired resistance (SAR) in dicots, there was no comparable SAR response to *F. graminearum* in barley. This study expands our knowledge about SA biosynthesis in barley and proves that SA confers basal resistance to fungal pathogens.

Keywords: *Hordeum vulgare*, isochorismate synthase, phenylalanine ammonia-lyase, systemic acquired resistance.

*Correspondence: Email: xuqian@sdau.edu.cn & dlfu@uidaho.edu
†These authors contributed equally to this work.
‡*Present address*: College of Biological Sciences, China Agricultural University, Beijing 100193, China

INTRODUCTION

Salicylic acid (SA) is a small phenolic compound that plays an important role in plant immunity (An and Mou, 2011), plant growth and development (Gallego-Giraldo *et al.*, 2011; Rivas-San Vicente and Plasencia, 2011). To date, the majority of studies, particularly those on eudicot species, have classified SA as a defence-related plant hormone.

Plants possess complex mechanisms to cope with both biotic and abiotic factors in nature. To respond to invading pathogens, plants have evolved two cross-talking defence cascades: pathogen-associated molecular pattern (PAMP)-triggered immunity (PTI), which confers basal resistance, and effector-triggered immunity (ETI), which induces the expression of resistance (*R*) genes (Dodds and Rathjen, 2010). Both PTI and ETI promote the accumulation of reactive oxygen species (ROS) (Yoshioka *et al.*, 2015). For biotrophic pathogens, ETI effectively limits pathogen spread by inducing a hypersensitive response (HR) at the site of pathogen entry (Jones and Dangl, 2006).

Systemic acquired resistance (SAR) is an induced systemic resistance after a pathogen has infected a plant locally (Fu and Dong, 2013). SAR is activated by several phloem-mobile signals, e.g. methyl salicylate (MeSA), dicarboxylic acid, azelaic acid (AzA) and jasmonic acid (JA) (Dempsey and Klessig, 2012; Fu and Dong, 2013), which form two SAR-inducing branches: one mediated by SA and its signalling component *NON-EXPRESSER OF PATHOGENESIS-RELATED GENE 1* (*NPR1*), and the other mediated by several free radicals, specifically nitric oxide (NO), ROS and AzA (Gao *et al.*, 2015). Once operational, SAR promotes the accumulation of pathogenesis-related (PR) proteins to confer disease resistance.

SA is synthesized via the isochorismate synthase (ICS)- and/or phenylalanine ammonia-lyase (PAL)-based branches of the shikimic acid pathway (Gao *et al.*, 2015; Sadeghi *et al.*, 2013; Vlot *et al.*, 2009; Wildermuth *et al.*, 2001). For example, tobacco can synthesize SA via the PAL branch (Lee *et al.*, 1995), and *Arabidopsis* can synthesize SA via the ICS branch (Abreu and Munné-Bosch, 2009; Wildermuth *et al.*, 2001). Both PAL and ICS branches

are important for pathogen-induced SA synthesis in soybean (Shine *et al.*, 2016). In *Arabidopsis*, there are two *ICS* genes, of which *ICS1* accounts for 90% of the SA products induced by pathogens or UV light (Garcion *et al.*, 2008). Both SA production and pathogen resistance are severely compromised in the *ics1* mutant (Garcion *et al.*, 2008). However, there are still some SA products in the *ics1/ics2* double mutant in *Arabidopsis* (Garcion *et al.*, 2008). SA is normally stored as inactive derivatives that can be converted back to free SA at the site of action. MeSA is a volatile SA derivative that is converted back to SA to induce SAR in the distal tissues between 48 and 72 h after primary infection (Gao *et al.*, 2015).

Fusarium graminearum causes the destructive Fusarium head blight (FHB) in wheat and barley. The fungus infects florets, spreads to adjacent spikelets, and causes necrosis and bleaching of the infected spikelets (Goswami and Kistler, 2004). SA provides basal resistance to multiple pathogens (Murray *et al.*, 2007; Thomma *et al.*, 1998). For example, SA confers both local and systemic defence responses to virus infection in tobacco (Yalpani *et al.*, 1991, 1993). The disruption of SA biosynthesis in *Arabidopsis* causes an increased susceptibility to *F. graminearum* (Makandar *et al.*, 2010). Similarly, in wheat, SA treatments have been shown to induce resistance to *F. graminearum* through a process that involves the increased expression of a number of anti-pathogen genes, including *PR1* (Makandar *et al.*, 2012). SA treatments can also cause disease-mimicking lesion formation in wheat in the absence of any pathogen (Anand *et al.*, 2003). In *Arabidopsis*, *NPR1* causes SAR, and the expression of *Arabidopsis NPR1* in wheat confers improved resistance to *F. graminearum* (Makandar *et al.*, 2006). However, there are very few reports of a cisgenic study of SA biosynthesis and disease resistance in Triticeae.

Here, we use barley, which is both an economically important cereal and a model member of the Triticeae family, to answer three questions about SA biosynthesis and its function in the Triticeae. (i) Can SA be synthesized by the ICS branch? (ii) Does SA contribute to basal resistance to *F. graminearum*? (iii) Does SA mediate SAR to the hemibiotrophic pathogen?

RESULTS

Low levels of SA promote plant growth

A gradient of SA, from 10 to 500 μM, was supplied during barley germination. Interestingly, although low levels of SA (10–100 μM, 50 μM in particular) promoted germination, and shoot and root growth, high levels of SA (200–500 μM) suppressed germination and plant growth (Fig. 1). Based on this complex response, SA appears to function as a growth factor or phytohormone in barley.

ICS and *PAL* are differentially organized in barley

As in rice (Yuan *et al.*, 2009), barley has a single *ICS* gene (GenBank AK358208; Table S1, see Supporting Information). The barley *ICS* gene is located on chromosome 5H and is orthologous to the rice *ICS* gene on chromosome 9. The cDNA of barley *ICS* is approximately 1.7 kb and is derived from 15 exons. The ICS proteins of barley, rice and *Brachypodium* share 77%–85% identity, but they show less than 51% identity when compared with the ICS proteins of *Arabidopsis* (Fig. 2a). Despite this, the ICS proteins of *Arabidopsis*, barley and rice fold into a similar predicted three-dimensional structure (Fig. S1a, see Supporting Information), suggesting a similar function.

There are multiple *PAL* genes in *Arabidopsis*, barley, *Brachypodium* and rice (Fig. 2b). The *Arabidopsis PAL* genes are more divergent from those in grasses. In barley, at least 10 *PAL* genes are found on chromosomes 1H, 2H and 6H (Table S1). The barley *PAL* genes are highly conserved with two exons and an approximate length of 2.1 kb, and their protein products share approximately 90% identity. Seven barley *PAL* genes form an independent clade similar to *OsPAL6*, but *HvPAL1* (AK253101), *HvPAL2* (AK356545) and *HvPAL3* (AK251356) were grouped in other clades with *Brachypodium* and rice homologues (Fig. 2b). The barley proteins have an alanine-serine-glycine (Ala-Ser-Gly) peptide (Fig. S1b) similar to the sequence found in the active site of other PAL proteins (Calabrese *et al.*, 2004).

ICS probably accounts for SA biosynthesis in barley

The barley *ICS* displayed ubiquitous expression in leaves, stem and sheath, but relatively low expression in spikes (Fig. 3a), suggesting that the plant's demands for SA might differ in different tissues. In the barley database, the *ICS* transcripts are also enriched in leaf tissue, but poorly represented in spikes, inflorescences or developing grains (Fig. S2, see Supporting Information). The seven *PAL* genes selected showed an equally biased organ-specific pattern of expression. Although the expression pattern of each *PAL* gene was unique, all showed lower expression in flag leaves (Figs 3b–f and S3, see Supporting Information). For example, *PAL1* is enriched in spikes, whereas *PAL6-4* and *PAL6-6* are enriched in stems. *PAL6-1* displays poor expression in the current study and in the barley database (Figs 3 and S2). Collectively, the expression of *PAL* genes was organ specific, most probably because of organ-specific differences in the flux of *trans*-cinnamic acid through secondary metabolism.

To study the function of *ICS* and *PAL* genes, we prepared both overexpression (OE) and RNA interference (RNAi) constructs (Fig. 4a), and transformed them into barley 'Golden Promise' (Table S2, see Supporting Information). Because the barley *ICS* is a single-copy gene, complete or near-complete silencing of this gene could be deleterious. As a precaution, we employed two different promoters to express *ICS* RNAi. The maize Ubiquitin (*Ubi*)

Fig. 1 Low concentrations of salicylic acid (SA) promote seedling growth in barley. Golden Promise seeds were treated with a gradient of SA (0–500 μM) for 1 week, when the photographs were taken. The micromolar (μM) concentration is indicated for each treatment. Scale bar, 1 cm.

promoter (Christensen *et al.*, 1992) is a constitutive promoter widely used in research. The wheat *Wks1* promoter (Fu *et al.*, 2009), on the other hand, is an alternative promoter that has been successfully used to express transgenes (Yuan *et al.*, 2018). All of the remaining constructs derived from the *ICS* and *PAL* genes were based on the *Ubi* promoter. All OE transgenic plants were generated using standard protocols. In the T_1 generation, plants segregated for the target transgene (Table S3, see Supporting Information). Except for *Wks1::ICS*$_{RNAi2}$, most transgenic plants were comparable with non-transgenic controls in terms of flowering time, tiller number and other tangible agronomic traits (Table S4, see Supporting Information). They behaved similarly in the T_2 generation (Fig. 4b). For RNAi studies, we generated transgenic plants for six *PAL* genes using standard procedures. The PAL6-6 construct actually targeted both *PAL6-6* and *PAL6–7*. All of the *PAL* RNAi plants were morphologically comparable with the non-transgenic control. However, we were unable to produce RNAi plants for the *ICS* gene using the established transformation procedure (Table S2). Both callus proliferation and plantlet regeneration were arrested, probably because the silencing of *ICS* led to inadequate SA to sustain normal cellular activity on the medium. We then modified the medium composition by the addition of 100 μM SA. As expected, the SA supplement partially rescued transgenic *ICS*$_{RNAi}$ cells, allowing them to proliferate and regenerate (Table S2). T_0 *ICS*$_{RNAi}$ plantlets, once established in soil, managed to flower and to set seed when they were supplied with water containing 100 μM SA. In the T_1 generation, additional SA was not essential to allow *ICS*$_{RNAi}$ plants to flower and set seed. The overexpression and silencing of three target genes were validated in the tested T_1 plants using quantitative real-time polymerase chain reaction (qRT-PCR) (Fig. S4, see Supporting Information). Based on these observations, the *ICS* gene probably accounts for the majority of SA biosynthesis in barley.

For the *ICS* gene, we obtained at least 11 independent OE lines, all employing the *Ubi* promoter. We only obtained three independent RNAi lines: one with *Ubi* and two with *Wks1* promoters (Table S2). In order to limit the breadth of the follow-up studies, we focused on two representative OE lines (*Ubi::ICS*$_{OE1}$ and *Ubi::ICS*$_{OE2}$) and two representative RNAi lines (*Ubi::ICS*$_{RNAi1}$ and *Wks1::ICS*$_{RNAi2}$) (Table S3). Except for the *Wks1::ICS*$_{RNAi2}$ line, all displayed a simple Mendelian segregation for one transgene in the T_1 generation (Table S3). Further phenotyping showed that

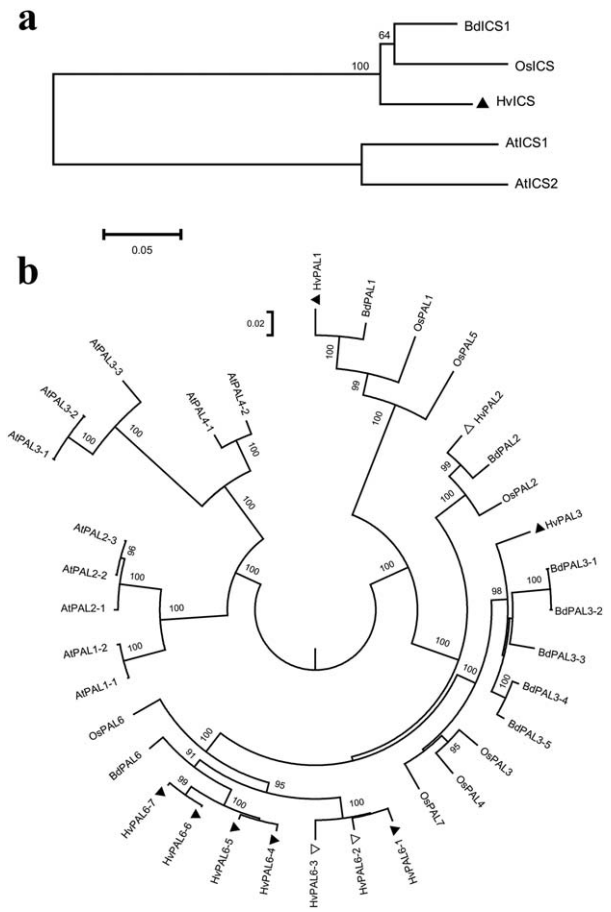

Fig. 2 Phylogenetic analysis of isochorismate synthase (ICS) and phenylalanine ammonia-lyase (PAL) proteins in barley. Phylogenetic trees of ICS (a) and PAL (b). We aligned the protein entries using CLUSTALW in MEGA6.06 (Tamura *et al.*, 2013), removed poor alignments on terminal regions and constructed a neighbour-joining tree with 1000 bootstrap iterations. The distance scale bar indicates amino acid differences per unit length. Bootstrap numbers above 50 and 80 are shown for ICS and PAL, respectively. The nomenclature of *PAL* is based on the rice homologues (Tonnessen *et al.*, 2015). Barley *PALs* are highlighted by triangles (▲ or Δ), and a solid triangle (▲) indicates a *PAL* gene under investigation. Protein alignment refers to Figs S1, S10 and S11 (see Supporting Information). Abbreviations: At, *Arabidopsis thaliana*; Bd, *Brachypodium distachyon*; Hv, *Hordeum vulgare*; Os, *Oryza sativa*. GenBank Accession Numbers: AtICS1 (AAL17715), AtICS2 (ACC60228), BdICS (XM_010239787), HvICS (AK358208), OsICS (AK120689), AtPAL1-1 (AY045919), AtPAL1–2 (XM002881442), AtPAL2-1 (XM002877863), AtPAL2-2 (NM115186), AtPAL2–3 (AY092957), AtPAL3-1 (NM120505), AtPAL3-2 (NM001203294), AtPAL3-3 (XM002871035), AtPAL4-1 (NP187645), AtPAL4-2 (XM002882616), BdPAL1 (XM003575348), BdPAL2 (XM003575352), BdPAL3-1 (XM003575190), BdPAL3-2 (XM003575192), BdPAL3-3 (XM003575355), BdPAL3–4 (XM003575356), BdPAL3–5 (XM003575317), BdPAL6 (XM003580096), HvPAL1 (AK253101), HvPAL2 (AK356545), HvPAL3 (AK251356), HvPAL6-1 (AK248831), HvPAL6-2 (AK361880), HvPAL6-3 (AK371460), HvPAL6-4 (AK249266), HvPAL6-5 (AK248841), HvPAL6-6 (AK250690), HvPAL6–7 (AK250100), OsPAL1 (Os02g41630), OsPAL2 (Os02g41650), OsPAL3 (Os02g41670), OsPAL4 (Os02g41680), OsPAL5 (Os04g43760), OsPAL6 (Os04g43800) and OsPAL7 (Os05g35290).

both *Ubi::ICS*$_{OE1}$ and *Ubi::ICS*$_{OE2}$ lines were comparable in many key measures of this study. Similarly, the *Ubi::ICS*$_{RNAi1}$ line was comparable with plants of the *Wks1::ICS*$_{RNAi2}$ line. Of the three spike lines of *Wks1::ICS*$_{RNAi2}$ (Table S3), both the W4- and W6-derived plants were comparable in plant height ($P = 0.6$) and tiller number ($P = 0.7$) in the T_1 generation. We then selected the spike line W4–8 as the representative source material for *Wks1::ICS*$_{RNAi}$. In the T_2 generation, we analysed plants of the *Ubi::ICS*$_{OE1}$ and *Wks1::ICS*$_{RNAi2}$ lineages, but also documented data from the T_2 plants of *Ubi::ICS*$_{OE2}$ and *Ubi::ICS*$_{RNAi1}$ in either the main text or Supporting Information.

We also prepared a tagged construct for *ICS:GFP* (Fig. 4a), and transformed it into *Brachypodium* 'Bd21-3'. In transgenic *Brachypodium*, ICS:GFP was localized to the chloroplast (Fig. 4c), which indicates that SA is most probably synthesized in chloroplasts in grass species as it is in *Arabidopsis* (Garcion *et al.*, 2008).

ICS regulates SA content and responsive genes in barley

In barley, overexpression increased the *ICS* mRNA by about 16- to 18-fold in T_2 plants (e.g. *Ubi::ICS*$_{OE1}$ and *Ubi::ICS*$_{OE2}$ derived from independent calli; Table S3) compared with endogenous *ICS* in wild-type controls (Fig. 4d). Interestingly, this correlated with a comparatively small increase in SA in T_2 plants (e.g. 24 ppb in *Ubi::ICS*$_{OE1}$; 1 ppb = 1 ng/g) compared with the WT control (15 ppb). As described above, we used both the *Ubi* and *Wks1* promoters to express *ICS* RNAi. It appeared that both *Ubi*- and *Wks1*-based RNAi reduced the *ICS* mRNA in T_2 plants (e.g. *Ubi::ICS*$_{RNAi1}$ and *Wks1::ICS*$_{RNAi2}$ derived from independent calli; Table S3) to about 49% (in *Wks1::ICS*$_{RNAi2}$) to 73% (in *Ubi::ICS*$_{RNAi1}$) of that in the WT control (Fig. 4d). However, the reduction was lower than that in the T_1 generation, which was about 13%–20% of that in the WT control (Fig. S4). Presumably, the recipient plants have certain mechanisms to counteract the engineered RNAi. The SA content in the RNAi T_2 plants (e.g. *Wks1::ICS*$_{RNAi2}$) was 13 ppb, which was lower but comparable with that of the WT control (e.g. 15 ppb). Collectively, the expression of *ICS* correlated with the SA content in barley, but evidently was not the only gene product responsible for the determination of SA accumulation and turnover.

Even these somewhat moderate perturbations in SA metabolism had a significant impact on the expression of SA-regulated genes. Using *ICS*-based transgenic barley, we examined *NPR1*, which encodes an SA signal transducer in *Arabidopsis* (Pieterse and Van Loon, 2004), *ERF1*, which encodes a positive regulator for disease resistance in JA/ethylene (ET) pathways (Lorenzo *et al.*, 2003), and *WRKY38*, which encodes a repressor targeting both SA and JA signalling (Kim *et al.*, 2008; Vlot *et al.*, 2009). The barley *NPR1* was not responsive to the level of expression of the *ICS*

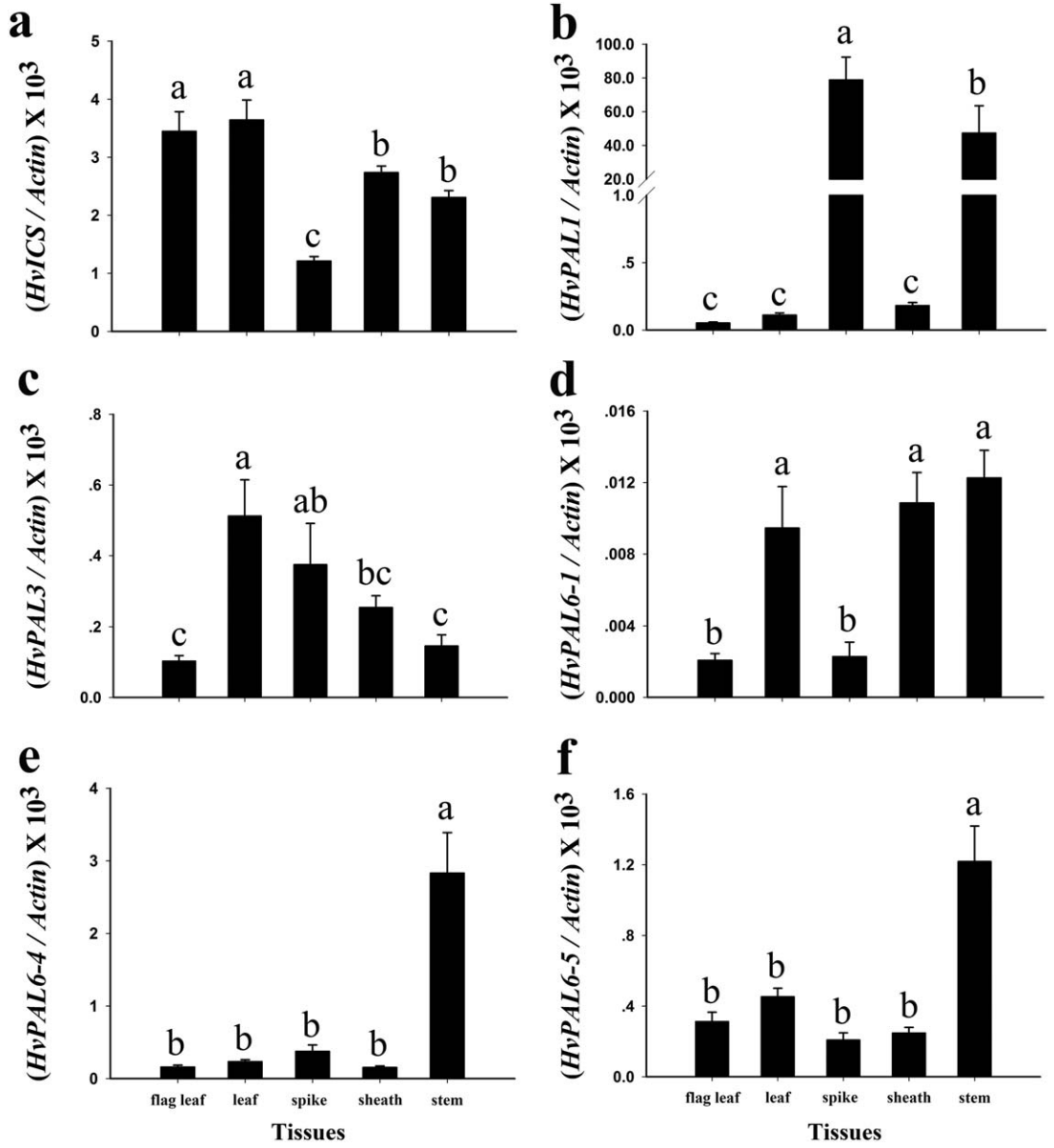

Fig. 3 Expression of *ICS* and *PAL* genes in barley. The mRNA expression of *HvICS* (a), *HvPAL1* (b), *HvPAL3* (c), *HvPAL6-1* (d), *HvPAL6-4* (e) and *HvPAL6-5* (f). The expression of these genes was analysed in the wild-type 'Golden Promise' at the heading stage. The tested organs were the flag leaf, penultimate leaf (leaf), peduncle (stem), sheath of the flag leaf (sheath) and inflorescence (spike). All measurements were normalized to the expression of *Actin*. Using SAS version 9.0 (SAS Institute Inc., Cary, NC, USA), comparisons were made using Duncan multiple range tests at a significance level of 0.05. Error bars represent the standard error of the mean (SEM).

gene, but *ERF1* and *WRKY38* displayed a negative correlation with the mRNA content of *ICS* (Fig. 4e).

Suppression of barley *ICS* compromises foliar resistance to *F. graminearum*

Fusarium graminearum causes FHB in wheat and barley; it is a necrotic pathogen, but with a biotrophic phase (Kazan *et al.*, 2012). Using a leaf-based test, we compared the *F. graminearum* lesions on infected leaves at 72 h post-inoculation (hpi). The RNAi T_2 plants (e.g. *Wks1::ICS*$_{RNAi2}$) showed the largest lesions, but those on the OE line (*Ubi::ICS*$_{OE1}$) were comparable with those on the WT control (Fig. 5a,b). The silencing of *ICS* compromised the basal resistance levels to *F. graminearum* in barley. We also tested the RNAi T_2 plants for their responses to *Blumeria graminis* f. sp. *hordei*, which is a biotrophic pathogen. At 5 days post-inoculation

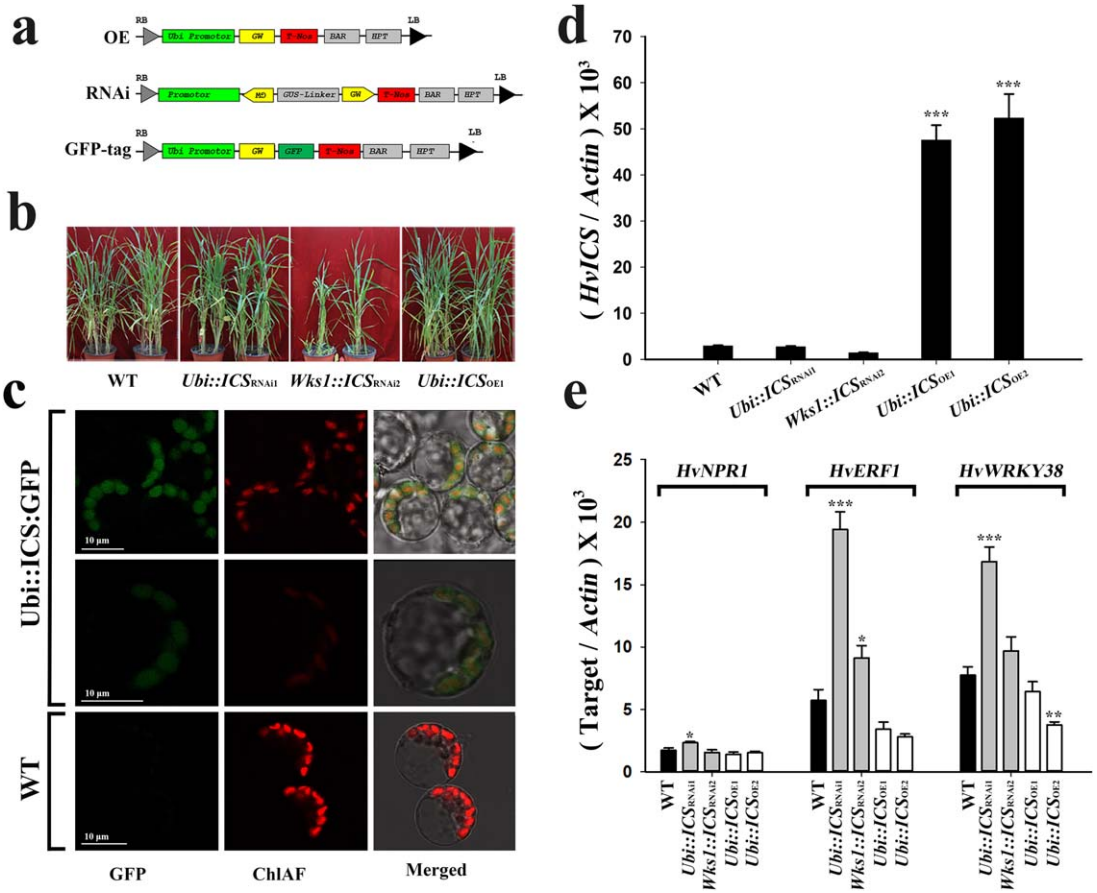

Fig. 4 Characterization of transgenic barley plants for the *ICS* gene. (a) Maps of the T-DNAs used to make constructs to overproduce (OE), silence (RNAi) or GFP-tag the target genes. (b) Typical phenotypes of wild-type (WT) barley, and transgenic T_2 barley with the *ICS* gene. (c) Subcellular localization of ICS-GFP and autofluorescing chlorophyll (ChlAF) in transgenic T_1 *Brachypodium* (top two rows). (d) The expression of *ICS* in transgenic T_2 barley with the *ICS* gene. (e) The expression of *HvNPR1*, *HvERF1* and *HvWRKY38* in transgenic T_2 barley with altered expression of *ICS*. The overexpression (OE) and RNA interference (RNAi) vectors were used for the *ICS* and *PAL* genes, but the green fluorescent protein (GFP) tag vector was only used for the *ICS* gene. The maize Ubiquitin (*Ubi*) promoter (Christensen *et al.*, 1992) and the wheat *Wks1* promoter (Fu *et al.*, 2009) were used to express the RNAi matrix. The *Ubi::ICS*$_{RNAi1}$ and *Wks1::ICS*$_{RNAi2}$ plants were derived from the *Ubi-* and *Wks1*-based constructs, respectively. All measurements were normalized to the expression of *Actin*. Comparisons were made using Dunnett's tests (transgenic lines vs. WT; $*P < 0.05$, $**P < 0.01$, $***P < 0.001$). Error bars are the standard error of the mean (SEM). GenBank Accession Numbers: *NPR1* (AM050559), *ERF1* (AK354662) and *WRKY38* (AK360269).

(dpi), the RNAi T_2 plants (e.g. *Wks1::ICS*$_{RNAi2}$) showed longer mycelia relative to those of the other lines (Fig. S5, see Supporting Information).

In *Arabidopsis*, pathogen infection induces expression levels of the *ICS1* gene (Wildermuth *et al.*, 2001). Similarly, *F. graminearum* infection in barley at 72 hpi up-regulates the expression of *ICS* (Fig. 5c), *NPR1* and *WRKY38* (Fig. S6, see Supporting Information). For all three tested genes, the OE line (*Ubi::ICS*$_{OE1}$) displayed the highest up-regulation ratio (2 : 1) when compared with the RNAi line (*Wks1::ICS*$_{RNAi2}$) and the WT control. In the infected tissue at 72 hpi, we also found that *F. graminearum* infection increased the localized SA content in the OE line (*Ubi::ICS*$_{OE1}$) and the WT control (Fig. 5d). The WT control was unexpectedly high with regard to localized SA. It remains unknown what caused an acute increase in SA in the WT control. However, the RNAi T_2 plant (e.g. *Wks1::ICS*$_{RNAi2}$) retained a low SA content despite *F. graminearum* infection (Fig. 5d). Apparently, barley ICS regulates the SA content under pathogen attack and, as a result, leads to higher defensive responses.

Overexpression of barley *ICS* enhances floral resistance to *F. graminearum*

Using a green fluorescent protein (GFP)-labelled strain, we then tested the floral responses to *F. graminearum* on transgenic plants with the *ICS* gene. The OE line (*Ubi::ICS*$_{OE1}$) was associated with the least fluorescence relative to the RNAi T_2 plants and WT control at an early infection stage (e.g. 24 and 48 hpi, Fig. 6a).

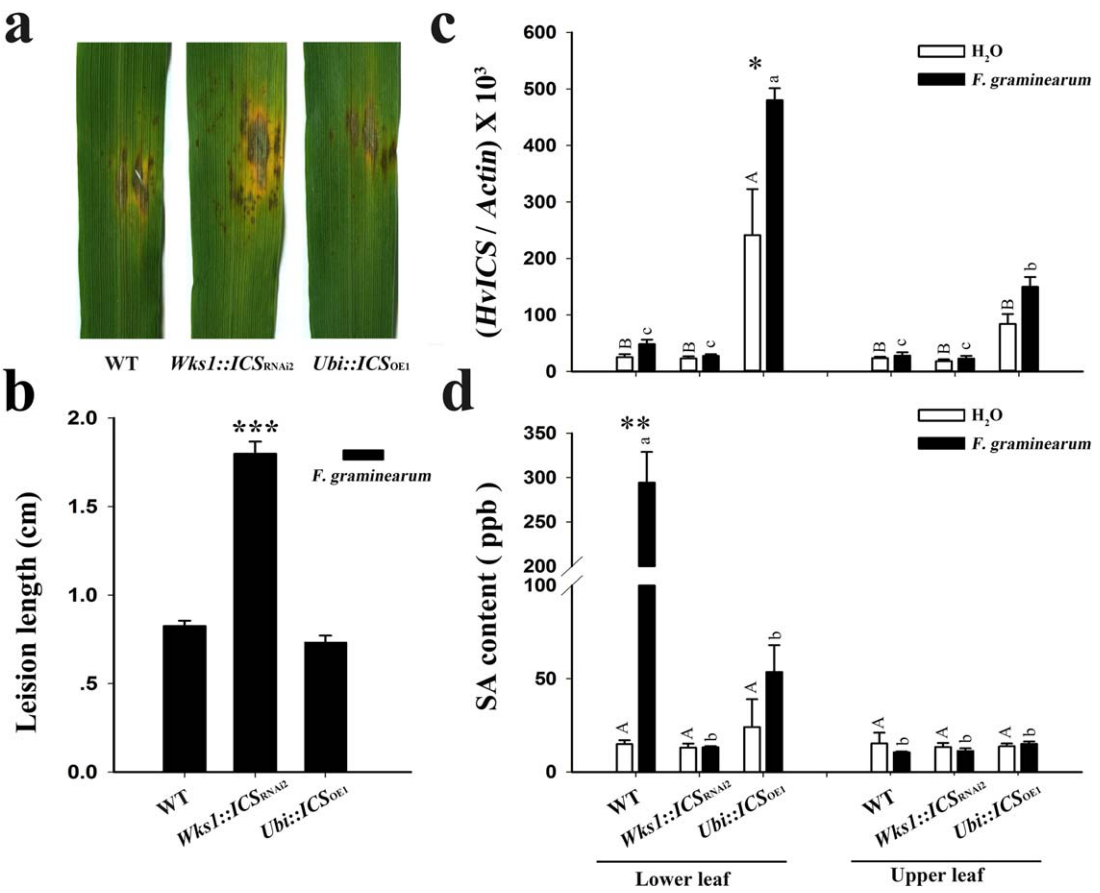

Fig. 5 *ICS* impacts barley foliar resistance to *Fusarium graminearum*. This figure illustrates lesion formation by *F. graminearum* on barley leaves (a), the length of developing lesions (b, $n = 10$), the mRNA level of *ICS* (c, $n = 6$) and the salicylic acid (SA) content (d, $n = 3$) in the wild-type (WT) and T_2 transgenic plants at 72 h post-inoculation (hpi). In (c) and (d), the lower leaves were treated using water or AmCyanPH-1; the upper leaves were untreated; the samples in (c) are arranged in the same order as those in (d). Dunnett's tests were used to compare transgenic vs. WT plants in (b), and the H_2O- vs. AmCyanPH-1-treated samples in (c) and (d) ($*P < 0.05$, $**P < 0.01$, $***P < 0.001$). Duncan's multiple range tests were used to compare the H_2O-treated samples (capital letters at $P < 0.05$) and the AmCyanPH-1-treated samples (small letters at $P < 0.05$) in (c) and (d). *Actin* was used as the internal control. Error bars are the standard error of the mean (SEM). Relative data of independent transgenic events refer to Fig. S12 (see Supporting Information).

However, there was no significant difference between the OE plants and other lines at the late infection stage (e.g. 72 hpi, Fig. 6a). We then estimated *F. graminearum* growth by quantification of the integrated fluorescence intensity (IFI) of the infected florets. Again, the OE plant was associated with the lowest IFI reading at 24 and 48 hpi ($P < 0.001$), but not at 72 hpi (Fig. 6b). Therefore, barley *ICS*, when overexpressed (Fig. 6c), enhances floral resistance to *F. graminearum*, but only during the initial stages of infection.

ICS modulates antioxidant enzymes and ROS in *Fusarium*-infected barley

ROS are responsive to pathogen infection (Torres *et al.*, 2006). We estimated the levels of superoxide radical (O_2^-) and hydrogen peroxide (H_2O_2) in *F. graminearum*-infected spikes from transgenic barley with altered *ICS* expression. After inoculation, the OE plant (e.g. *Ubi::ICS*$_{OE1}$) was lighter in colour when stained with diaminobenzidine (DAB) (Fig. 7a) and nitroblue tetrazolium (NBT) (Fig. 7b) than the WT control. This indicated that there were lower concentrations of O_2^- and H_2O_2 in the OE plant when compared with the unaltered plant. We further confirmed this pattern by quantifying the content of H_2O_2 and the O_2^- production rate in different genotypes (Fig. 7c,d). We then estimated the activity of antioxidant enzymes. The OE plant (e.g. *Ubi::ICS*$_{OE1}$) was associated with higher activity of ascorbate peroxidase (APX), catalase (CAT), guaiacol peroxidase (POD) and superoxide dismutase (SOD) at both the infection site (central spikelet) and in an uninfected site (upper spikelet) (Fig. 8). APX and SOD showed maximum expression at 24 hpi, but CAT and POD (of the upper spikelet) peaked at 72 hpi. It is likely that higher activities of antioxidant enzymes were responsible for reducing O_2^- and H_2O_2 accumulation in the

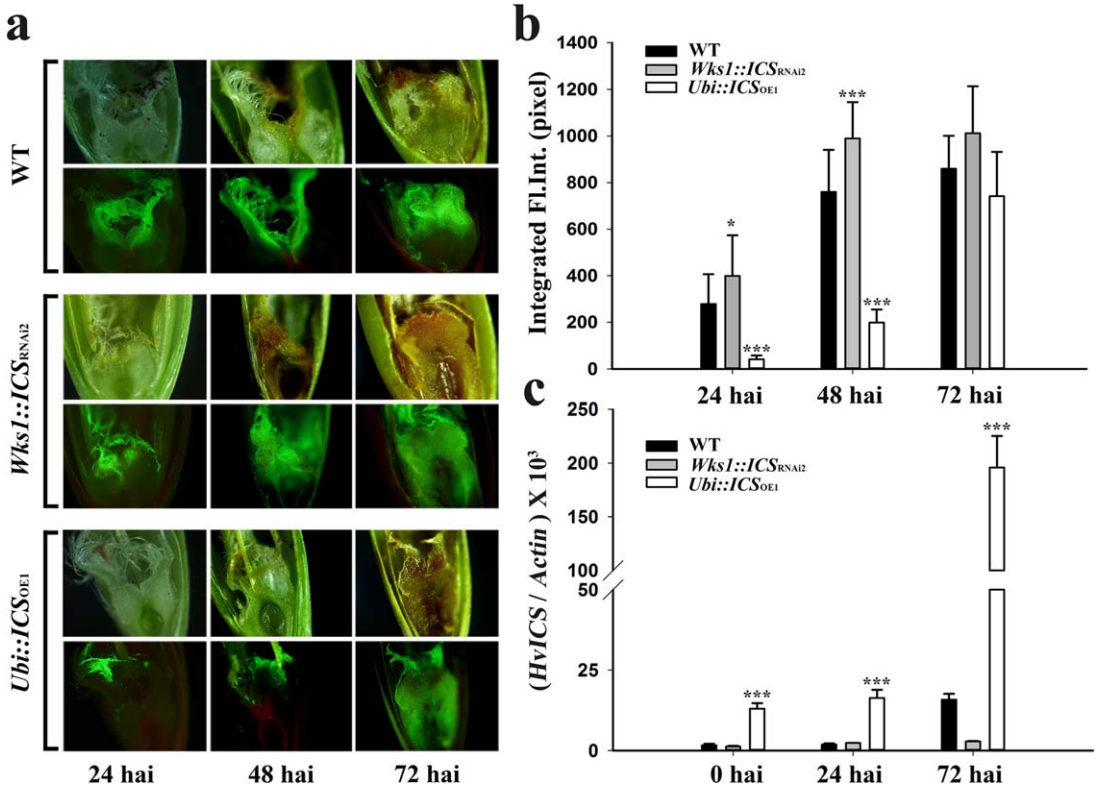

Fig. 6 *ICS* regulates floral resistance to Fusarium head blight (FHB) in T_2 transgenic barley. (a) AmCyanPH-1-based green fluorescence in infected florets of three barley lines labelled on the left. Each line was photographed in both bright field (top images of each set) and fluorescence (bottom images of each set). (b) Integrated fluorescence intensity (Integrated Fl. Int.) of the infected florets: at least 10 florets were analysed for each genotype using ImageJ. (c) The expression of *ICS* in infected florets. Tukey–Kramer's tests plus a pdiff option were used to compare transgenic vs. wild-type (WT) plants in (b), and Dunnett's tests were used to compare transgenic vs. WT plants in (c) ($*P < 0.05$, $***P < 0.001$). *Actin* was used as the internal control. Error bars are the standard error of the mean (SEM). Relative data of independent transgenic events refer to Fig. S13 (see Supporting Information). hai, hours after inoculation.

OE plants (e.g. *Ubi::ICS*$_{OE1}$). However, the RNAi plants either accumulated WT, or less than WT, levels of APX, CAT, POD and SOD (except for the upper spikelet at 72 hpi) (Figs 7 and 8).

SAR is not significant in barley

SA plays an important role in SAR in numerous plants (Vlot *et al.*, 2009). In barley, exogenous SA reduces *Fusarium* seedling blight (Wiśniewska and Chełkowski, 1999). However, whether SA induces a practical SAR to one or multiple pathogens in barley remains to be answered. In order to investigate this, we examined the expression of some relevant genes and measured the SA content at a primary *F. graminearum* infection site and at an uninfected site (upper leaves). In the primary infection site, *ICS* expression in the OE plant (e.g. *Ubi::ICS*$_{OE1}$) was up-regulated when compared with the H_2O control. No such up-regulation occurred in *Wks1::ICS*$_{RNAi2}$ (Fig. 5c). *NPR1* and *WRKY38* similarly showed increased expression at the primary infection sites in OE plants (Fig. S6a,b). However, in uninfected sites, only *WRKY38*, and not *ICS* and *NPR1*, showed a significant increase in expression in OE plants (Figs 5c and S6a,b). Silencing of the *ICS* gene abolished the systemic up-regulation of *ICS*, *NPR1* and *WRKY38*.

We then compared the hormone contents at both primary infected and secondary uninfected sites. At the primary infection site, *F. graminearum* triggered an increase in SA content in the WT, but not in the RNAi and OE genotypes (Fig. 5d). These same infections appeared to increase JA in all genotypes, but not abscisic acid (ABA) (Fig. S6c,d). However, comparable increases in the hormones did not occur at the secondary uninfected site (Figs 5d and S6c,d). Phenotypically, SAR was also not detected on barley leaves tested with *F. graminearum* (Fig. S7, see Supporting Information).

DISCUSSION

SA is an essential hormone in barley development

In plants, SA is normally classified as a signal molecule that promotes anti-pathogen defences in plants (An and Mou, 2011). However, SA also plays an important role in abiotic adaptation,

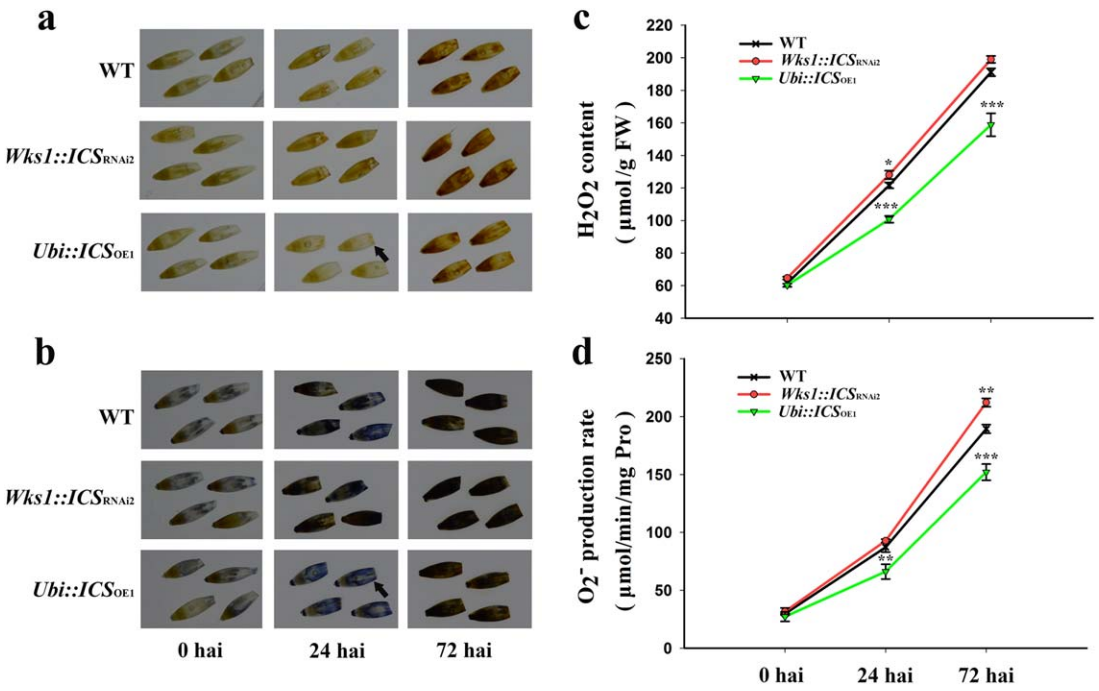

Fig. 7 Accumulation of reactive oxygen species in T_2 transgenic barley after *Fusarium graminearum* infection. (a) Diaminobenzidine (DAB) staining for H_2O_2. (b) Nitroblue tetrazolium (NBT) staining for O_2^-. (c) Increase in H_2O_2 levels over 72 h after infection (hai). (d) Increased rate of production of O_2^- over 72 hai. Dunnett's tests were used to compare transgenic vs. wild-type (WT) plants (*$P < 0.05$, **$P < 0.01$, ***$P < 0.001$). Arrows indicate a low stain in the *Ubi::ICS*$_{OE1}$ plant at 24 hai. Error bars are standard error of the mean (SEM). FW, fresh weight; hai, hours after inoculation; Pro, proline.

growth and development (Rivas-San Vicente and Plasencia, 2011). In this study, SA treatment significantly impacted seed growth in barley (Fig. 1). In *Arabidopsis*, low levels of endogenous SA led to increased leaf biomass production at the early stages of reproduction and increased seed yield in NahG-expressing transgenic lines and *sid2* mutants (Abreu and Munné-Bosch, 2009). In the current study, low levels of endogenous SA strongly delayed growth and flowering. For instance, RNAi-based repression of the *ICS* gene diminished the ability of transformed cells to regenerate. These transgenic cells could be rescued by supplementation of their medium with 100 μM SA. However, how the *ICS* RNAi progenies (T_1 and T_2) bypassed the need for SA supplementation in order to grow, flower and set seed remains unclear. It appears that tissue culture and regeneration are more sensitive than the whole plant to the effects of SA reduction. It was noted that, although the RNAi plants developed without SA-supplied watering, *Wks1::ICS*$_{RNAi2}$ plants appeared to be slow in germination (Fig. S8, see Supporting Information) and in the other developmental processes. Similarly, a knock-out of the *ICS-A* locus led to dwarfism and late flowering in the durum wheat 'Kronos' (Fig. S9, see Supporting Information). Too much SA can also be inhibitory: the overaccumulation of SA caused a stunted rosette growth in *Arabidopsis* (Janda *et al.*, 2014). The present article shows that high levels of exogenous SA delay seed germination and shoot growth in barley (Fig. 1).

In *Arabidopsis*, chorismate is a substrate for producing isochorismate and, subsequently, SA through the actions of ICS and pyruvate lyase (Wildermuth *et al.*, 2001). Most pathogen-induced SA is synthesized by this pathway in *Nicotiana benthamiana* (Catinot *et al.*, 2008). *Arabidopsis* ICS1 accounts for approximately 90% of SA and its derivatives that are induced by pathogens or UV light (Garcion *et al.*, 2008). The barley ICS, encoded by a single gene, shares high similarity with the isoforms found in *Arabidopsis* and rice (*Orvza sativa*). The current study proposes that ICS is required to synthesize SA in barley, and probably in other grass species.

SA confers basal resistance to *F. graminearum* in barley

In *Arabidopsis*, *Erysiphe orontii* infection increased the SA content about five-fold (Wildermuth *et al.*, 2001). Similarly, *F. graminearum* infection resulted in extensive SA induction in wild-type barley (Fig. 5d). Unexpectedly, this induction was not seen in OE lines. Why the OE lines did not respond in a similar manner to WT barley remains unclear. Apparently, the SA pathway and its regulatory network are more complicated than expected, and it is already known that SA interacts with the biosynthetic pathways of other phytohormones (Robert-Seilaniantz *et al.*, 2011). Therefore, the conclusions of this study are viewed

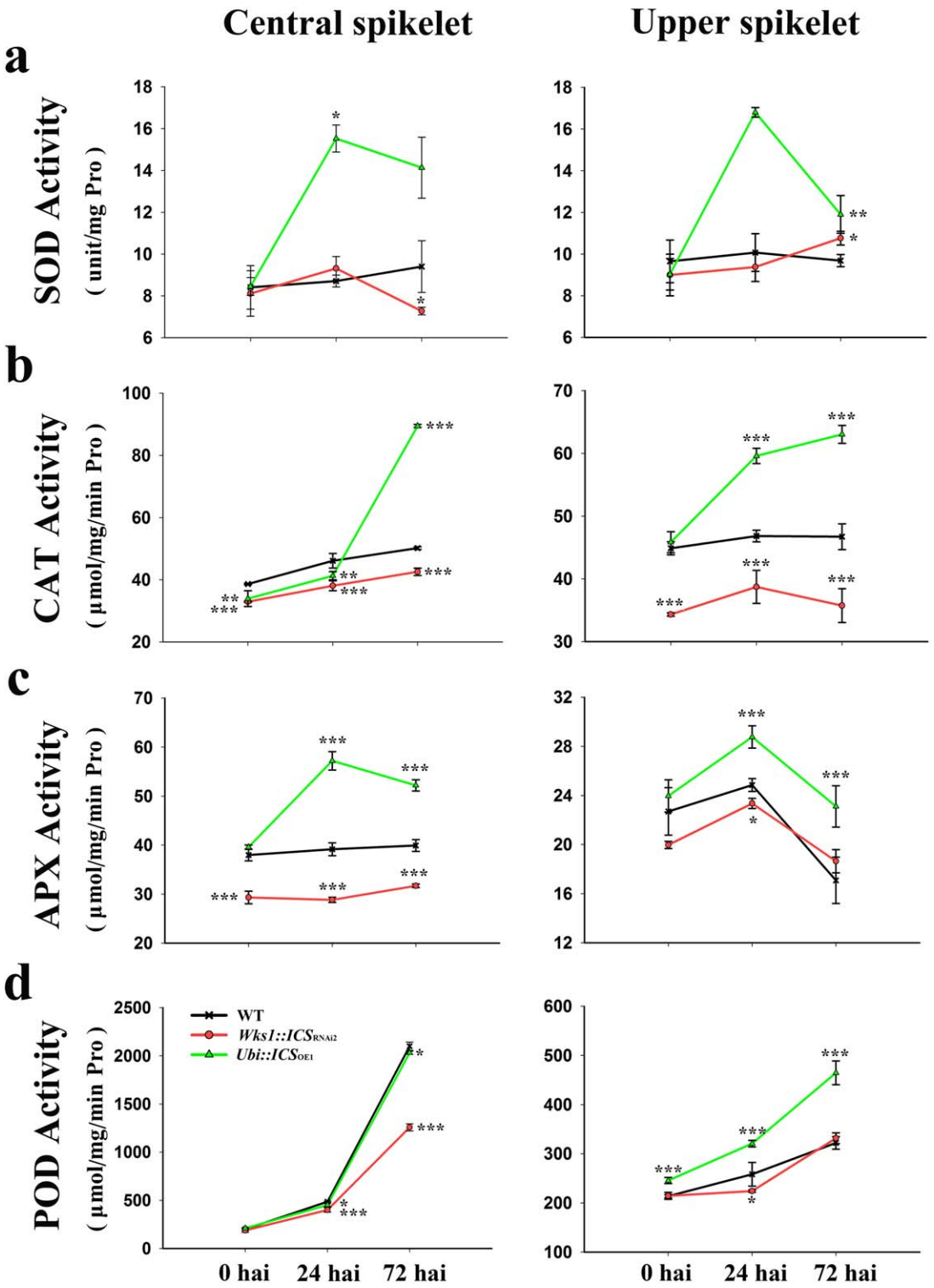

Fig. 8 Characterization of antioxidant enzymes in T_2 transgenic barley after *Fusarium* infection. Enzymatic activities of superoxide dismutase (SOD) (a), catalase (CAT) (b), ascorbate peroxidase (APX) (c) and guaiacol peroxidase (POD) (d). Central spikelets were inoculated with *F. graminearum*; upper spikelet represents a secondary uninfected site. Dunnett's tests were used to compare transgenic vs. wild-type (WT) plants (*$P < 0.05$, **$P < 0.01$, ***$P < 0.001$). Error bars are standard error of the mean (SEM). hai, hours after inoculation; Pro, proline.

as being based on the 'perturbation' of SA accumulation rather than on simple decreases/increases in SA levels.

In *Arabidopsis*, the expression of *ICS* positively responds to pathogen infection (Garcion *et al.*, 2008), consistent with the suggested role of SA biosynthesis in biotic stress responses. Here, we demonstrated that *F. graminearum* infection increased the SA content in the wild-type, but not in the *ICS*-silenced line (Fig. 5d). This suggests that barley synthesizes SA via an ICS-dependent pathway when responding to pathogen attack.

Traditionally, SA has been assumed to protect plants from biotrophic pathogens, whereas JA and ET protect plants from necrotrophic pathogens (Glazebrook, 2005). *Fusarium graminearum* is hemibiotrophic, that is, biotrophic initially, but necrotrophic during pathogenesis when cell death is induced (Kazan *et al.*, 2012). In wheat, *F. graminearum* 'true' resistance is probably mediated by JA and ET, and not SA (Li and Yen, 2008). However, SA contributes to this resistance by inhibiting mycelial growth and conidial germination of *F. graminearum* (Qi *et al.*, 2012). In the current study, overexpression of *ICS* increased SA concentration, which repressed the initial infection at 24 and 48 hpi (Fig. 6a), but had no significant effect on the repression of pathogenesis at a later stage of infection (Fig. 6a,b). Apparently, SA enhanced the basal resistance during the biotrophic stage of *F. graminearum* attack. Here, we have further confirmed that the down-regulation of SA biosynthesis promotes the growth of *Blumeria graminis* f. sp. *hordei* – a biotrophic pathogen. Therefore, SA regulates plant basal resistance to some biotrophic pathogens or to some pathogens at the biotrophic stages of their life cycle.

The accumulation of ROS is one of the earliest events in plants under pathogen attack. A ROS burst could be caused by or, through a feed-back loop, cause SA signalling (Chen *et al.*, 1993; Leon *et al.*, 1995). In this study, *ICS*-overexpressing lines were associated with higher antioxidant enzyme activity and lower levels of H_2O_2 and O_2^- than those in the wild-type controls and the *ICS*-silenced lines (Fig. 7c,d). However, how an improved antioxidant activity contributes to *F. graminearum* resistance remains unclear.

SAR is ineffective against *F. graminearum* in barley

SAR, as a form of broad-spectrum resistance, is induced in response to local infections and protects uninfected parts against subsequent secondary infections by related or unrelated pathogens (Singh *et al.*, 2017). SAR has been well documented in dicotyledonous plants (Fu and Dong, 2013; Vlot *et al.*, 2009), but is poorly understood in monocotyledonous plants.

In wheat, a number of reports have addressed SAR (Moya-Elizondo and Jacobsen, 2016; Plotnikova, 2009; Yang *et al.*, 2013). For example, foliar applications of *Bacillus mycoides* reduced the severity of Fusarium crown rot, which was assumed to be caused by *B. mycoides*-induced SAR (Moya-Elizondo and Jacobsen, 2016). In barley, foliar application of *Pseudomonas syringae* induced broad-spectrum acquired resistance (AR) at a distance from the local lesion (Colebrook *et al.*, 2012). Other studies using the biotrophic pathogen *Blumeria graminis* have revealed that the barley AR is strictly localized to the inoculated cell or to the cells immediately adjacent to the site of attempted penetration (Lyngkjær and Carver, 1999; Ouchi *et al.*, 1976). Because these results are so contradictory, it remains unclear whether a classic SAR protective against varied pathogens exists in this group of grasses.

To test the *F. graminearum* infection in barley, we performed a double inoculation procedure ('inducer' followed by 'challenger') (Lyngkjær and Carver, 1999). We found that the infection of the inducer on one leaf did not induce SAR against the challenger on a different leaf (Fig. S7). There was no significant change in *ICS* expression and SA level at uninfected sites (Fig. 5c,d), even though peroxidase activity was up-regulated at uninfected sites in the *ICS* OE line (Fig. 8). Thus, although barley appears to have a basal systemic defence response, as indicated by the detectable cellular responses of SAR at a secondary uninfected site, this is inadequate to confer a practical SAR for secondary infections, at least for *F. graminearum* tested here.

EXPERIMENTAL PROCEDURES

Plant material and *Fusarium* strain

This study was performed on spring barley (*Hordeum vulgare* L., cultivar 'Golden Promise') and purple false brome (*Brachypodium distachyon* L., inbred line 'Bd21-3'). Wild-type and transgenic plants were grown in glasshouses with a 16-h photoperiod (light intensity, 105 μmol/m^2/s) and a daytime temperature of 25 °C.

Fusarium tests were performed using the *F. graminearum* strain 'AmCyanPH-1', which is an engineered strain expressing the AmCyan fluorescent protein (Zhang *et al.*, 2012). AmCyanPH-1 was provided by Dr W. Tang (Shanghai Institutes for Biological Sciences, Chinese Academy of Sciences, Shanghai, China). Powdery mildew tests were performed using the *Blumeria graminis* f. sp. *hordei* isolate 'K1' (Liu *et al.*, 2014), which is virulent to Golden Promise. *Blumeria graminis* f. sp. *hordei* isolate K1 was provided by Dr Q. Shen (Institute of Genetics and Developmental Biology, Chinese Academy of Sciences, Beijing, China).

Plasmid construction

In barley, there is a single *ICS* gene (GenBank AK358208) and at least seven *PAL* homologues: *PAL1* (AK253101), *PAL3* (AK251356), *PAL6-1* (AK248831), *PAL6-4* (AK249266), *PAL6-5* (AK248841), *PAL6-6* (AK250690) and *PAL6-7* (AK250100). Their full-length cDNAs were isolated from the barley cultivar 'Tamalpais', and cloned into the Gateway (GW)-compatible OE vector PC186 (p*Ubi::GW$_{OE}$::Nos*). To trigger specific RNAi of *ICS*, the 80–385-bp region (counted from the start codon) was cloned into the RNAi vectors PC336 (*Ubi::GW$_{RNAi}$::Nos*) and PC691 (*Wks1::GW$_{RNAi}$::Nos*), where *Ubi*, *Wks1* and *Nos* are the maize *Ubi*

promoter (Christensen *et al.*, 1992), wheat *Wks1* gene promoter (Fu *et al.*, 2009) and *Agrobacterium Nos* terminator (Wood *et al.*, 2001), respectively. For *PAL* genes, we cloned a 1792–1990-bp region (counted from the start codon) into the RNAi vector PC336 (*Ubi::GW*$_{RNAi}$*::Nos*). The barley *ICS* gene was also cloned into the vector PC611 (*Ubi::GW:GFP:: Nos*), where it gained a C-terminal GFP. PCR primers are described in Table S5 (see Supporting Information).

Generation of transgenic plants

Agrobacterium-mediated barley transformation

Agrobacterium-mediated gene transfer was performed using the published protocol (Harwood *et al.*, 2009) with slight modifications. Plant expression constructs were first introduced into the *A. tumefaciens* strain 'AGL1' using electroporation. A single AGL1 colony was amplified in liquid MG/L medium containing 50 mg/L kanamycin, 40 mg/L rifampicin and 100 mg/L carbenicillin, and the culture was shaken at 200 rpm and 28 °C for 48 h. The AGL1 suspension, about 200 μL, was spread on solid MG/L medium with the same supplements, and set in a 28 °C incubator for 48 h. AGL1 colonies were suspended in liquid callus induction medium (CIM), adjusted to an optical density at 600 nm (OD_{600}) of 0.6, supplied with 200 μM acetosyringone and 0.1% (v/v) PE/F68 (Sigma, St Louis, MO, USA), and subjected to co-cultivation with barley explants.

To prepare immature embryos, caryopses were collected from developing spikes that were approximately 14 days post-pollination, sterilized in a solution of ethanol (75%, v/v) and Tween-20 (5%, v/v) for 5 min, plus an ultrasonic treatment at room temperature (stimulating time, 6 s; interval, 30 s; repeated six times), sterilized again in 20% (v/v) sodium hypochlorite for 15 min with shaking (200 rpm), and rinsed five times using sterile deionized water. Immature embryos (1.5–2.5 mm in length) were collected from sterilized caryopses using fine forceps; after removing the embryonic axis, immature embryos were placed with the scutellum side up onto CIM supplied with 2.5 mg/L Dicamba and incubated in the dark at 24 °C for 2 days.

A drop of 10 μL of fresh AGL1 inoculum (OD_{600} = 0.6) was added to the embryo scutellum. After the surface had been air dried (about 60 min at room temperature), the infected embryos (scutellum side up) were co-cultured on fresh CIM medium supplied with 2.5 mg/L Dicamba and 200 μM acetosyringone at 24 °C in the dark for 3 days, and then transferred to CIM medium supplemented with 200 mg/L Timentin and 25 mg/L hygromycin at 24 °C. The infected material was maintained in the dark, and subcultured every 14 days for a total of 12 weeks. During/after subculture, the most vigorously growing embryogenic callus was transferred to shoot induction medium (SIM) supplied with 2.5 mg/L 2,4-Dichlorophenoxyacetic acid (2,4-D), 0.1 mg/L 6-Benzylaminopurine (6-BA), 200 mg/L Timentin and 25 mg/L hygromycin, and incubated at 24 °C under 16 h of fluorescent light (light intensity, 2 μmol/m^2/s) for 2 weeks. Vigorous embryogenic callus with green tissue was moved to SIM medium supplemented with 200 mg/L Timentin and 25 mg/L hygromycin with no additional hormones, and incubated at 24 °C under 16 h of fluorescent light (light intensity, 25 μmol/m^2/s) for 3–4 weeks. Regenerated plantlets were transplanted to root induction medium (RIM). Plantlets with healthy roots were maintained in an open tissue culture bottle for 3 days, and then transferred to soil in a glasshouse.

Transgenic plants were confirmed by PCR amplification of the selection markers (*BAR* or *HPT*) and/or vector-specific fragments. Transgenic plants were also wipe tested for their resistance to 0.3% (v/v) Finale herbicide (undiluted herbicide containing 11.33% glufosinate ammonium). The T_2 transgenic plants were prioritized for the current study.

Agrobacterium-mediated transformation in Brachypodium

Tissue culture and *Agrobacterium*-mediated transformation of *Brachypodium* were conducted as reported by Bragg *et al.* (2012).

Quantitative transcription analysis

Total RNA was extracted using Trizol reagent (Life Technologies, Grand Island, NY, USA). cDNA was synthesized using a Fermentas First Strand cDNA Synthesis Kit (Thermo Scientific, Waltham, MA, USA). For qRT-PCR, primer efficiency (93–100%, Table S5) was tested on 10-fold serial dilutions of cDNA templates using StepOnePlus Systems (Life Technologies) and FastStart SYBR Green Master (Roche Applied Science, Indianapolis, IN, USA). qRT-PCR cycles were 10 min at 95 °C, 40 cycles of two consecutive steps of 15 s at 95 °C and 1 min at 60 °C, and a standard dissociation procedure. Quantitative transcription was averaged from six biological replicates. *Actin* and *Cyclophilin* were used as endogenous controls (Table S5).

Measurement of SA and JA contents

An established procedure (Xu *et al.*, 2016) was used to quantify SA and JA in barley leaves and spikes. About 150 mg of fresh leaves or spikes were harvested and ground in liquid nitrogen for analysis. Hormones were extracted in 1.9 mL of 70% acetone: 30% 50 mM citric acid solution supplemented with 10 ng each of the internal standards dihydrojasmonic acid (Sigma) and [$^2H_4$]-SA (Olchemim, Olomouc, Czech Republic). After removing acetone by overnight evaporation, samples were re-extracted with diethyl ether. Dry samples were resuspended in methanol, filtered through a 0.22-mm Polyvinylidene fluoride (PVDF) membrane (Millipore, Bedford, MA, USA) and analysed using a liquid chromatography–tandem mass spectrometry system (TSQ Quantiva, Thermo Fisher Scientific, Waltham, MA, USA) with an optimized ion source. Each compound and its internal standard were quantified by tandem mass spectrometry using the scan mode at *m/z* 137.12 (SA) and 141.27 ([$^2H_4$]-SA), 209.3 (JA) and 211.09 (dihydrojasmonic acid). Electrospray ionization (ESI) analysis was performed in negative ionization mode. Each extraction and analysis were replicated four times.

Subcellular localization

Transgenic *Brachypodium* plants with a GFP tag were germinated in a dark chamber at 28 °C. Protoplasts were isolated from 2-week-old seedlings using a published protocol (Hong *et al.*, 2012). In brief, the first two leaves were excised and cut at intervals of 0.1 mm using a sharp razor blade. Leaf cuts were immediately soaked in 20 mL of filter-sterilized solution containing 0.6 M mannitol, 10 mM 2-(N-morpholino)ethanesulfonic acid (MES, pH 5.7), 1.5% cellulase 'Onozuka R-10' (Yakult Pharmaceutical, Tokyo, Japan), 0.75% macerozyme 'R-10' (Yakult Pharmaceutical), 0.1% bovine serum albumin, 1 mM $CaCl_2$ and 5 mM β-mercaptoethanol. A vacuum (–68.95 kPa) was applied for 30 min to enhance enzyme filtration

into the tissues. The leaf–enzyme mixture was first shaken at 40 rpm in the dark at room temperature for 3 h, and was then shaken at 60 rpm for 30 min to release the protoplasts. Protoplasts were inspected under a Leica TCS SP5 II laser scanning confocal microscope (Leica Microsystems, Wetzlar, Hesse, Germany).

Accumulation of superoxide radicals (O_2^-) and hydrogen peroxide (H_2O_2)

The accumulation of O_2^- and H_2O_2 in leaves was visually evaluated by staining with NBT (0.5 mg/mL, pH 7.6) for O_2^- and DAB (1 mg/mL, pH 3.8) for H_2O_2. Chlorophyll was removed by infiltrating leaves with lactol–glycerol–ethanol (1 : 1 : 4, v/v/v).

The concentration of O_2^- was measured as reported previously (Sui *et al.*, 2007). Leaf tissues were thoroughly ground in potassium phosphate buffer (50 mM, pH 7.8) on ice. A 0.5-mL aliquot of supernatant was removed and mixed with 0.5 mL of phosphate buffer (50 mM, pH 7.8) and 1 mL of 10 mM hydroxylammonium chloride. The mixture was incubated at 25 °C for 20 min. Finally, 4 mL of ethyl ether was added to the mixture. The absorbance of the water phase was measured at 530 nm. The content of H_2O_2 was determined by estimating the titanium-hydroperoxide complex (Mukherjee and Choudhuri, 1983).

Antioxidant enzyme activity

The activities of selected enzymes were determined as described previously, including SOD (He *et al.*, 2005), APX (Cakmak and Marschner, 1992), CAT (Durner and Klessig, 1996) and POD (Scebba *et al.*, 2001). Enzymatic activity was quantified using a UV–visible spectrophotometer (UV-2550, Shimadzu, Japan) at 25 °C.

Fusarium graminearum test

Both leaf- and spike-based tests were performed. The harvested conidia were resuspended in sterile water and adjusted to 10^7/mL. For the leaf-based bioassay, the conidial suspension was pressure infiltrated with a needle-less syringe on the abaxial side to produce a 15-mm-long water-soaked area. The infiltrated leaf was enclosed in a size-compatible plastic bag with wet cotton to maintain 100% humidity. The lesion length was measured at 4 dpi using the ImageJ program (ImageJ 1.44p, Wayne Rasband, National Institutes of Health, Bethesda, MD, USA; http://imagej.nih.gov/ij).

For the spike-based bioassay, 10 μL of fresh conidial suspension (10^6/mL) was added between the lemma and palea in the middle florets of a spike (Kang and Buchenauer, 1999), whereas the control plants were mock inoculated with distilled water. After inoculation, wheat heads were misted with water and covered with plastic bags to maintain high humidity for 72 h. For each fungal strain, two independent experiments were performed. At least six barley heads were examined in each replicate. Green fluorescence was observed at 24, 48, 72 and 96 hpi.

To test SAR in barley, we performed a double inoculation procedure ('inducer' followed by 'challenger') (Lyngkjær and Carver, 1999). Three experiments were designed: (I) inducer of *F. graminearum* on lower leaves and challenger of *F. graminearum* on upper leaves; (II) inducer of *F. graminearum* on upper leaves and challenger of *F. graminearum* on lower leaves; and (III) inducer of *F. graminearum* on middle leaves of tiller one and challenger of *F. graminearum* on middle leaves of tiller two. Water 'inducer' controls and *F. graminearum* 'challenger' were performed separately. The challenger infection was conducted 4 days after the inducer treatment on the same plant. Experiments were repeated 10 times, with one replication per plant.

Powdery mildew bioassay

Barley seedlings at the tillering stage were infiltrated with a solution of spores of *B. graminis* f. sp. *hordei* isolate K1 (density, 5 conidia/mm^2) (Lumbroso *et al.*, 1982), and maintained in a humid glasshouse for 3 days. Leaf tissues were then boiled for 10 min in a fresh solution containing phenol, lactic acid, glycerol and distilled water (1 : 1 : 1 : 1, v/v/v/v) with 0.5 mg/mL trypan blue, and maintained at room temperature for 6–8 h. Leaf tissues were then clarified overnight in 2.5 mg/mL chloral hydrate. Leaf samples were examined using an Olympus BX50 light microscope (Olympus, Tokyo, Japan).

Phylogenetic analysis

Phylogenetic analysis was performed on the protein sequences. The program MEGA 6.06 (Tamura *et al.*, 2013) was used to align entries, to remove InDels and to construct a neighbour-joining tree with 1000 bootstrap iterations. The distance scale bar indicates the amino acid differences per unit length. Bootstrap numbers above 80 and 50 are shown for PAL and ICS, respectively.

ACKNOWLEDGEMENTS

We thank Dr Weihua Tang for kindly providing the *F. graminearum* strain AmCyanPH-1 and Dr Qianhua Shen for providing *Blumeria graminis* f. sp. *hordei* isolate K1. We also thank Dr Lynn Epstein for reviewing the manuscript. This work was supported by the National Key Research and Development Program of China (2016YFD0100602 and 2016YFD0101004), the National Key Basic Research Program in China (2013CB1277002), the Hatch project IDA01587 and the Agriculture and Food Research Initiative Competitive Grant 2017-67007-25939 from the USDA National Institute of Food and Agriculture. There were no conflicts of interest.

REFERENCES

Abreu, M.E. and Munné-Bosch, S. (2009) Salicylic acid deficiency in *NahG* transgenic lines and *sid2* mutants increases seed yield in the annual plant *Arabidopsis thaliana*. *J. Exp. Bot.* **60**, 1261–1271.

An, C. and Mou, Z. (2011) Salicylic acid and its function in plant immunity. *J. Integr. Plant Biol.* **53**, 412–428.

Anand, A., Schmelz, E.A. and Muthukrishnan, S. (2003) Development of a lesion-mimic phenotype in a transgenic wheat line overexpressing genes for pathogenesis-related (PR) proteins is dependent on salicylic acid concentration. *Mol. Plant–Microbe Interact.* **16**, 916–925.

Bragg, J.N., Wu, J., Gordon, S.P., Guttman, M.E., Thilmony, R., Lazo, G.R., Gu, Y.Q. and Vogel, J.P. (2012) Generation and characterization of the Western Regional Research Center Brachypodium T-DNA insertional mutant collection. *PLoS One*, **7**, e41916.

Cakmak, I. and Marschner, H. (1992) Magnesium deficiency and high light intensity enhance activities of superoxide dismutase, ascorbate peroxidase, and glutathione reductase in bean leaves. *Plant Physiol.* **98**, 1222–1227.

Calabrese, J.C., Jordan, D.B., Boodhoo, A., Sariaslani, S. and Vannelli, T. (2004) Crystal structure of phenylalanine ammonia lyase: multiple helix dipoles implicated in catalysis. *Biochemistry*, **43**, 11 403–11 416.

Catinot, J., Buchala, A., Abou-Mansour, E. and Métraux, J.-P. (2008) Salicylic acid production in response to biotic and abiotic stress depends on isochorismate in *Nicotiana benthamiana*. *FEBS Lett.* **582**, 473–478.

Chen, Z., Silva, H. and Klessig, D. (1993) Active oxygen species in the induction of plant systemic acquired resistance by salicylic acid. *Science*, **262**, 1883–1886.

Christensen, A.H., Sharrock, R.A. and Quail, P.H. (1992) Maize polyubiquitin genes: structure, thermal perturbation of expression and transcript splicing, and promoter activity following transfer to protoplasts by electroporation. *Plant Mol. Biol.* **18**, 675–689.

Colebrook, E.H., Creissen, G., McGrann, G.R.D., Dreos, R., Lamb, C. and Boyd, L.A. (2012) Broad-spectrum acquired resistance in barley induced by the *Pseudomonas* pathosystem shares transcriptional components with *Arabidopsis* systemic acquired resistance. *Mol. Plant–Microbe Interact.* **25**, 658–667.

Dempsey, D.M.A. and Klessig, D.F. (2012) SOS – too many signals for systemic acquired resistance? *Trends Plant Sci.* **17**, 538–545.

Dodds, P.N. and Rathjen, J.P. (2010) Plant immunity: towards an integrated view of plant–pathogen interactions. *Nat. Rev. Genet.* **11**, 539–548.

Durner, J. and Klessig, D.F. (1996) Salicylic acid is a modulator of tobacco and mammalian catalases. *J. Biol. Chem.* **271**, 28 492–28 501.

Fu, D., Uauy, C., Distelfeld, A., Blechl, A., Epstein, L., Chen, X., Sela, H., Fahima, T. and Dubcovsky, J. (2009) A kinase-START gene confers temperature-dependent resistance to wheat stripe rust. *Science*, **323**, 1357–1360.

Fu, Z. and Dong, X. (2013) Systemic acquired resistance: turning local infection into global defense. *Annu. Rev. Plant Biol.* **64**, 839–863.

Gallego-Giraldo, L., Escamilla-Trevino, L., Jackson, L.A. and Dixon, R.A. (2011) Salicylic acid mediates the reduced growth of lignin down-regulated plants. *Proc. Natl. Acad. Sci. USA*, **108**, 20 814–20 819.

Gao, Q.-M., Zhu, S., Kachroo, P. and Kachroo, A. (2015) Signal regulators of systemic acquired resistance. *Front. Plant Sci.* **6**, 228.

Garcion, C., Lohmann, A., Lamodiere, E., Catinot, J., Buchala, A., Doermann, P. and Metraux, J.-P. (2008) Characterization and biological function of the *ISOCHORISMATE SYNTHASE2* gene of *Arabidopsis*. *Plant Physiol.* **147**, 1279–1287.

Glazebrook, J. (2005) Contrasting mechanisms of defense against biotrophic and necrotrophic pathogens. *Annu. Rev. Phytopathol.* **43**, 205–227.

Goswami, R.S. and Kistler, H.C. (2004) Heading for disaster: *Fusarium graminearum* on cereal crops. *Mol. Plant Pathol.* **5**, 515–525.

Harwood, W.A., Bartlett, J.G., Alves, S.C., Perry, M., Smedley, M.A., Leyland, N. and Snape, J.W. (2009) Barley transformation using *Agrobacterium*-mediated techniques. In: *Transgenic Wheat, Barley and Oats: Production and Characterization Protocols* (Jones, D. H. and Shewry, R. P., eds), pp. 137–147. Totowa, NJ: Humana Press.

He, P., Osaki, M., Takebe, M., Shinano, T. and Wasaki, J. (2005) Endogenous hormones and expression of senescence-related genes in different senescent types of maize. *J. Exp. Bot.* **56**, 1117–1128.

Hong, S.-Y., Seo, P.J., Cho, S.-H. and Park, C.-M. (2012) Preparation of leaf mesophyll protoplasts for transient gene expression in *Brachypodium distachyon*. *J. Plant Biol.* **55**, 390–397.

Janda, M., Šašek, V. and Ruelland, E. (2014) The *Arabidopsis* pi4kIIIβ1β2 double mutant is salicylic acid-overaccumulating: a new example of salicylic acid influence on plant stature. *Plant Signal. Behav.* **9**, e977210.

Jones, J.D.G. and Dangl, J.L. (2006) The plant immune system. *Nature*, **444**, 323–329.

Kang, Z. and Buchenauer, H. (1999) Immunocytochemical localization of fusarium toxins in infected wheat spikes by *Fusarium culmorum*. *Physiol. Mol. Plant Pathol.* **55**, 275–288.

Kazan, K., Gardiner, D.M. and Manners, J.M. (2012) On the trail of a cereal killer: recent advances in *Fusarium graminearum* pathogenomics and host resistance. *Mol. Plant Pathol.* **13**, 399–413.

Kim, K.-C., Lai, Z., Fan, B. and Chen, Z. (2008) *Arabidopsis* WRKY38 and WRKY62 transcription factors interact with histone deacetylase 19 in basal defense. *Plant Cell*, **20**, 2357–2371.

Krasileva, K.V., Vasquez-Gross, H.A., Howell, T., Bailey, P., Paraiso, F., Clissold, L., Simmonds, J., Ramirez-Gonzalez, R.H., Wang, X., Borrill, P., Fosker, C., Ayling, S., Phillips, A.L., Uauy, C. and Dubcovsky, J. (2017) Uncovering hidden variation in polyploid wheat. *Proc. Natl. Acad. Sci. USA*, **114**, E913–E921.

Lee, H.I., León, J. and Raskin, I. (1995) Biosynthesis and metabolism of salicylic acid. *Proc. Natl. Acad. Sci. USA*, **92**, 4076–4079.

Leon, J., Lawton, M.A. and Raskin, I. (1995) Hydrogen peroxide stimulates salicylic acid biosynthesis in tobacco. *Plant Physiol.* **108**, 1673–1678.

Li, G. and Yen, Y. (2008) Jasmonate and ethylene signaling pathway may mediate Fusarium head blight resistance in wheat. *Crop Sci.* **48**, 1888–1896.

Liu, J., Cheng, X., Liu, D., Xu, W., Wise, R. and Shen, Q.-H. (2014) The miR9863 family regulates distinct *Mla* alleles in barley to attenuate NLR receptor-triggered disease resistance and cell-death signaling. *PLOS Genet.* **10**, e1004755.

Lorenzo, O., Piqueras, R., Sánchez-Serrano, J.J. and Solano, R. (2003) ETHYLENE RESPONSE FACTOR1 integrates signals from ethylene and jasmonate pathways in plant defense. *Plant Cell*, **15**, 165–178.

Lumbroso, E., Fischbeck, G. and Wahl, I. (1982) Infection of barley with conidia suspensions of *Erysiphe graminis* f. sp. *hordei*. *J. Phytopathol.* **104**, 222–233.

Lyngkjær, M.F. and Carver, T.L.W. (1999) Induced accessibility and inaccessibility to *Blumeria graminis* f.sp. *hordei* in barley epidermal cells attacked by a compatible isolate. *Physiol. Mol. Plant Pathol.* **55**, 151–162.

Makandar, R., Essig, J.S., Schapaugh, M.A., Trick, H.N. and Shah, J. (2006) Genetically engineered resistance to Fusarium head blight in wheat by expression of *Arabidopsis* NPR1. *Mol. Plant–Microbe Interact.* **19**, 123–129.

Makandar, R., Nalam, V., Chaturvedi, R., Jeannotte, R., Sparks, A.A. and Shah, J. (2010) Involvement of salicylate and jasmonate signaling pathways in *Arabidopsis* interaction with *Fusarium graminearum*. *Mol. Plant–Microbe Interact.* **23**, 861–870.

Makandar, R., Nalam, V.J., Lee, H., Trick, H.N., Dong, Y. and Shah, J. (2012) Salicylic acid regulates basal resistance to Fusarium head blight in wheat. *Mol. Plant–Microbe Interact.* **25**, 431–439.

Moya-Elizondo, E.A. and Jacobsen, B.J. (2016) Integrated management of Fusarium crown rot of wheat using fungicide seed treatment, cultivar resistance, and induction of systemic acquired resistance (SAR). *Biol. Control.* **92**, 153–163.

Mukherjee, S.P. and Choudhuri, M.A. (1983) Implications of water stress-induced changes in the levels of endogenous ascorbic acid and hydrogen peroxide in *Vigna* seedlings. *Physiol. Plant.* **58**, 166–170.

Murray, S.L., Ingle, R.A., Petersen, L.N. and Denby, K.J. (2007) Basal resistance against *Pseudomonas syringae* in *Arabidopsis* involves WRKY53 and a protein with homology to a nematode resistance protein. *Mol. Plant–Microbe Interact.* **20**, 1431–1438.

Ni, F., Qi, J., Hao, Q., Lyu, B., Luo, M.-C., Wang, Y., Chen, F., Wang, S., Zhang, C., Epstein, L., Zhao, X., Wang, H., Zhang, X., Chen, C., Sun, L. and Fu, D. (2017) Wheat *Ms2* encodes for an orphan protein that confers male sterility in grass species. *Nat. Commun.* **8**, 15 121.

Nicholas, K.B., Nicholas, H.B. Jr. and Deerfield, D.W. II. (1997) GeneDoc: Analysis and visualization of genetic variation. *Embnet News* **4**, 1–4.

Ouchi, S., Oku, H. and Hibino, C. (1976) Localization of induced resistance and susceptibility in barley leaves inoculated with the powdery mildew fungus. *Phytopathology*, **66**, 901–905.

Pieterse, C.M.J. and Van Loon, L.C. (2004) NPR1: the spider in the web of induced resistance signaling pathways. *Curr. Opin. Plant Biol.* **7**, 456–464.

Plotnikova, L.Y. (2009) Effect of benzothiadiazole, an inducer of systemic acquired resistance, on the pathogenesis of wheat brown rust. *Russ. J. Plant Physiol.* **56**, 517–526.

Qi, P.-F., Johnston, A., Balcerzak, M., Rocheleau, H., Harris, L.J., Long, X.-Y., Wei, Y.-M., Zheng, Y.-L. and Ouellet, T. (2012) Effect of salicylic acid on *Fusarium graminearum*, the major causal agent of fusarium head blight in wheat. *Fungal Biol.* **116**, 413–426.

Rivas-San Vicente, M. and Plasencia, J. (2011) Salicylic acid beyond defence: its role in plant growth and development. *J. Exp. Bot.* **62**, 3321–3338.

Robert-Seilaniantz, A., Grant, M. and Jones, J.D.G. (2011) Hormone crosstalk in plant disease and defense: more than just jasmonate–salicylate antagonism. *Annu. Rev. Phytopathol.* **49**, 317–343.

Sadeghi, M., Dehghan, S., Fischer, R., Wenzel, U., Vilcinskas, A., Kavousi, H.R. and Rahnamaeian, M. (2013) Isolation and characterization of isochorismate synthase and cinnamate 4-hydroxylase during salinity stress, wounding, and salicylic acid treatment in *Carthamus tinctorius*. *Plant Signal. Behav.* **8**, e27335.

Scebba, F., Sebastiani, L. and Vitagliano, C. (2001) Activities of antioxidant enzymes during senescence of *Prunus armeniaca* leaves. *Biol. Plant.* **44**, 41–46.

Shine, M.B., Yang, J.-W., El-Habbak, M., Nagyabhyru, P., Fu, D.-Q., Navarre, D., Ghabrial, S., Kachroo, P. and Kachroo, A. (2016) Cooperative functioning between phenylalanine ammonia lyase and isochorismate synthase activities contributes to salicylic acid biosynthesis in soybean. *New Phytol.* **212**, 627–636.

Singh, A., Lim, G.-H. and Kachroo, P. (2017) Transport of chemical signals in systemic acquired resistance. *J. Integr. Plant Biol.* **59**, 336–344.

Sui, N., Li, M., Liu, X.-Y., Wang, N., Fang, W. and Meng, Q.-W. (2007) Response of xanthophyll cycle and chloroplastic antioxidant enzymes to chilling stress in tomato over-expressing glycerol-3-phosphate acyltransferase gene. *Photosynthetica*, **45**, 447–454.

Tamura, K., Stecher, G., Peterson, D., Filipski, A. and Kumar, S. (2013) MEGA6: molecular evolutionary genetics analysis version 6.0. *Mol. Biol. Evol.* **30**, 2725–2729.

Thomma, B.P.H.J., Eggermont, K., Penninckx, I.A.M.A., Mauch-Mani, B., Vogelsang, R., Cammue, B.P.A. and Broekaert, W.F. (1998) Separate jasmonate-dependent and salicylate-dependent defense-response pathways in *Arabidopsis* are essential for resistance to distinct microbial pathogens. *Proc. Natl. Acad. Sci. USA*, **95**, 15 107–15 111.

Tonnessen, B.W., Manosalva, P., Lang, J.M., Baraoidan, M., Bordeos, A., Mauleon, R., Oard, J., Hulbert, S., Leung, H. and Leach, J.E. (2015) Rice phenylalanine ammonia-lyase gene *OsPAL4* is associated with broad spectrum disease resistance. *Plant Mol. Biol.* **87**, 273–286.

Torres, M.A., Jones, J.D.G. and Dangl, J.L. (2006) Reactive oxygen species signaling in response to pathogens. *Plant Physiol.* **141**, 373–378.

Vlot, A.C., Dempsey, D.M.A. and Klessig, D.F. (2009) Salicylic acid, a multifaceted hormone to combat disease. *Annu. Rev. Phytopathol.* **47**, 177–206.

Wildermuth, M.C., Dewdney, J., Wu, G. and Ausubel, F.M. (2001) Isochorismate synthase is required to synthesize salicylic acid for plant defence. *Nature*, **414**, 562–565.

Wiśniewska, H. and Chełkowski, J. (1999) Influence of exogenic salicylic acid on *Fusarium* seedling blight reduction in barley. *Acta Physiol. Plant.* **21**, 63–66.

Wood, D.W., Setubal, J.C., Kaul, R., Monks, D.E., Kitajima, J.P., Okura, V.K., Zhou, Y., Chen, L., Wood, G.E., Almeida, NF. Jr., Woo, L., Chen, Y., Paulsen, I.T., Eisen, J.A., Karp, P.D., Bovee, D. Sr., Chapman, P., Clendenning, J., Deatherage, G., Gillet, W., Grant, C., Kutyavin, T., Levy, R., Li, M.J., McClelland, E., Palmieri, A., Raymond, C., Rouse, G., Saenphimmachak, C., Wu, Z., Romero, P., Gordon, D., Zhang, S., Yoo, H., Tao, Y., Biddle, P., Jung, M., Krespan, W., Perry, M., Gordon-Kamm, B., Liao, L., Kim, S., Hendrick, C., Zhao, Z.Y., Dolan, M., Chumley, F., Tingey, S.V., Tomb, J.F., Gordon, M.P., Olson, M.V. and Nester, E.W. (2001) The genome of the natural genetic engineer *Agrobacterium tumefaciens* C58. *Science*, **294**, 2317–2323.

Xu, Q., Truong, T.T., Barrero, J.M., Jacobsen, J.V., Hocart, C.H. and Gubler, F. (2016) A role for jasmonates in the release of dormancy by cold stratification in wheat. *J. Exp. Bot.* **67**, 3497–3508.

Yalpani, N., Silverman, P., Wilson, T.M., Kleier, D.A. and Raskin, I. (1991) Salicylic acid is a systemic signal and an inducer of pathogenesis-related proteins in virus-infected tobacco. *Plant Cell*, **3**, 809–818.

Yalpani, N., Shulaev, V. and Raskin, I. (1993) Endogenous salicylic acid levels correlate with accumulation of pathogenesis-related proteins and virus resistance in tobacco. *Phytopathology*, **83**, 702–708.

Yang, Y., Zhao, J., Liu, P., Xing, H., Li, C., Wei, G. and Kang, Z. (2013) Glycerol-3-phosphate metabolism in wheat contributes to systemic acquired resistance against *Puccinia striiformis* f. sp. *tritici*. *PLoS One*, **8**, e81756.

Yoshioka, H., Adachi, H., Ishihama, N., Nakano, T., Shiraishi, Y., Miyagawa, N., Nomura, H., Yoshioka, M. and Asai, S. (2015) Molecular mechanisms of ROS burst conferred by protein phosphorylation. *Jpn. J. Phytopathol.* **81**, 1–8.

Yuan, C., Wu, J., Yan, B., Hao, Q., Zhang, C., Lyu, B., Ni, F., Caplan, A., Wu, J. and Fu, D. (2018) Remapping of the stripe rust resistance gene *Yr10* in common wheat. *Theor. Appl. Genet.* DOI: 10.1007/s00122-00018-03075-00129; https://doi.org/10.1007/s00122-018-3075-9

Yuan, Y., Chung, J.-D., Fu, X., Johnson, V.E., Ranjan, P., Booth, S.L., Harding, S.A. and Tsai, C.-J. (2009) Alternative splicing and gene duplication differentially shaped the regulation of isochorismate synthase in *Populus* and *Arabidopsis*. *Proc. Natl. Acad. Sci. USA*, **106**, 22 020–22 025.

Zhang, X.-W., Jia, L.-J., Zhang, Y., Jiang, G., Li, X., Zhang, D. and Tang, W.-H. (2012) In planta stage-specific fungal gene profiling elucidates the molecular strategies of *Fusarium graminearum* growing inside wheat coleoptiles. *Plant Cell*, **24**, 5159–5176.

SUPPORTING INFORMATION

Additional Supporting Information may be found in the online version of this article at the publisher's website:

Fig. S1 Protein structure of isochorismate synthase (ICS) and phenylalanine ammonia-lyase (PAL). (a) Predicted three-dimensional structure of ICS proteins. (b) The alanine-serine-glycine (Ala-Ser-Gly, ASG) signature of the identified PAL proteins. Proteins are from *Arabidopsis thaliana* (At), *Brachypodium distachyon* (Bd), *Hordeum vulgare* (Hv) and *Oryza sativa* (Os).

Fig. S2 Barley *ICS* and *PAL* transcripts in the IPK database. In the IPK server (http://webblast.ipk-gatersleben.de/barley_ibsc/viroblast.php), we searched for the *ICS* gene in the HC_genes_CDS_Seq_2012 database, and for the *PAL* genes in the Barley CDS HC May2016 database. The *x* axes (in b–g) share the same labels, and tissues were numbered from 1 to 16 as shown in (g). CAR5/CAR15, developing grain (5 or 15 DAP); EMB, 4-day embryo; EPI, epidermal strips (28 DAP); ETI, etiolated seedling, dark condition (10 DAP); FPKM, fragments per kilobase million; INF1/INF2, developing inflorescences (5 mm or 1–1.5 cm); LEA, shoots from seedlings (10-cm shoot stage); LEM/LOD, inflorescences, lemma (42 DAP) or lodicule (42 DAP); NOD, developing tillers, third internode (42 DAP); PAL/RAC, dissected inflorescences, palea (42 DAP) or rachis (35 DAP); ROO1/ROO2, roots (from 10-cm shoot stage or 28 DAP); SEN, senescing leaves (56 DAP). DAP, days after pollination.

Fig. S3 Expression of *PAL6-6* and *PAL6-7* in barley. *HvPAL6-6* and *HvPAL6-7* were collectively determined in 'Golden Promise' at the heading stage. The tested organs were the flag leaf, penultimate leaf (leaf), peduncle (stem), sheath of the flag leaf (sheath) and inflorescence (spike). All measurements were normalized to the expression of *Actin*. Differences between different parts of the plant were compared using Duncan's multiple range tests at a significance level of 0.05. Error bars represent the standard error of the mean (SEM).

Fig. S4 Expression of *ICS* and *PAL* in transgenic T_1 plants. In the T_1 generation, we measured the expression of *ICS*, *HvPAL1* and *HvPAL6-4* in the respective transgenic plants. The genetic background of the *PAL* transgenic lines is provided in Table S3. All measurements were normalized to the expression of *Cyclophilin*. Comparisons were made using Dunnett's tests [transgenic lines vs. wild-type (WT); $*P < 0.05$, $***P < 0.001$]. Error bars are the standard error of the mean (SEM).

Fig. S5 *ICS* affects powdery mildew resistance in barley. (a) Trypan blue staining of developing hyphae of *Blumeria graminis* f. sp. *hordei*. (b) Length of fungal hyphae in infected plants. Error bars represent the standard error of the mean (SEM). Tukey–Kramer's tests plus a pdiff option were used to compare hyphal length in the T_2 transgenic vs. wild-type (WT) plants ($**P < 0.01$). Scale bars, 100 μm (a).

Fig. S6 Gene expression and hormone accumulation in the *ICS*-based T_2 transgenic plants. This figure illustrates the expression of *HvNPR1* (a) and *HvWRKY* (b) and the content of jasmonic acid (JA) (c) and abscisic acid (ABA) (d) in wild-type and transgenic plants at 72 h post-inoculation (hpi). Samples in (a) were arranged in the same order as those in (b), and likewise for (c) and (d). Duncan's multiple range tests were used to compare the H_2O-treated samples (capital letters at $P < 0.05$) and AmCyanPH-1-treated samples (small letters at $P < 0.05$). Dunnett's tests were used to compare the H_2O- vs.

AmCyanPH-1-treated samples (*$P < 0.05$, **$P < 0.01$, ***$P < 0.001$). *Actin* was used as the internal control. Error bars are the standard error of the mean (SEM). Open bars, water control; black bars, *F. graminearum* infected.

Fig. S7 Barley leaves showing insignificant systemic acquired resistance (SAR) response to *Fusarium graminearum*. The figure illustrates necrotic spots (a) and lesion sizes (b, c). The three experiments were as follows: (I) inducer of *F. graminearum* (fg) or water (CK) on lower leaves (LL) and challenger of *F. graminearum* on upper leaves (UL); (II) inducer of *F. graminearum* or water on upper leaves and challenger of *F. graminearum* on lower leaves; and (III) inducer of *F. graminearum* or water on middle leaves of tiller one (TL1) and challenger of *F. graminearum* on middle leaves of tiller two (TL2). Inducer and challenger responses from the same plant are highlighted by labels with or without an underline. The challenger responses in each experiment were compared using Dunnett's tests. Error bars are the standard error of the mean (SEM).

Fig. S8 Germination of the transgenic T_2 seeds. Barley grains were hand-threshed and treated in tap water for 2 days at room temperature with 12 h light. WT, wild-type.

Fig. S9 *ICS* mutants of tetraploid wheat 'Kronos'. (a) Growth of the wild-type (WT) Kronos and two *ICS-A* mutants (3735, G593A, missense mutation; 2561, G1905A, splicing mutation). (b) TILLING (Targeting Induced Local Lesions IN Genomes) analysis of sister plants of the selected mutant lines. Among the sister plants, white and red IDs correspond to segregants with and without the target mutations, respectively. (c) Chlorophyll (Chl) content. (d) Plant height. (e) Heading date. The Kronos mutants were identified by blast search (Krasileva *et al.*, 2017) or by traditional TILLING (Ni *et al.*, 2017). Dunnett's tests were used to compare transgenic vs. WT plants in (c) (***$P < 0.001$). Tukey–Kramer's tests plus a pdiff option were used to compare transgenic vs. WT plants in (d) and (e) (*$P < 0.05$, ***$P < 0.001$). Error bars are the standard error of the mean (SEM). Scale bars, 10 cm (in a); M, DNA ladder (in b). Note that *ICS-A* mutants grew more slowly, matured to heading more slowly and, in the more severe mutant (2561), had less chlorophyll in their leaves. FW, fresh weight.

Fig. S10 Sequence alignment of the isochorismate synthase (ICS) proteins. Protein sequences were aligned using CustalW in MEGA6.06 (Tamura *et al.*, 2013) and illustrated by GeneDoc (Nicholas *et al.*, 1997). GenBank Accession Numbers refer to Fig. 2. At, *Arabidopsis thaliana*; Bd, *Brachypodium distachyon*; Hv, *Hordeum vulgare*; Os, *Oryza sativa*.

Fig. S11 Sequence alignment of the phenylalanine ammonia-lyase (PAL) proteins. Protein sequences were aligned using ClustalW in MEGA6.06 (Tamura *et al.*, 2013) and illustrated by GeneDoc. GenBank Accession Numbers refer to Fig. 2. At, *Arabidopsis thaliana*; Bd, *Brachypodium distachyon*; Hv, *Hordeum vulgare*; Os, *Oryza sativa*.

Fig. S12 *ICS* impacts barley foliar resistance to *Fusarium graminearum*. This figure illustrates lesion formation by *F. graminearum* on barley leaves (a), the length of developing lesions (b, $n = 10$) and the mRNA level of *ICS* (c, $n = 6$) in the wild-type (WT) and T_2 transgenic plants at 72 h post-inoculation (hpi). In (c), the lower leaves were treated using water or AmCyanPH-1; the upper leaves were untreated. Dunnett's tests were used to compare transgenic vs. WT plants in (b), and the H_2O- vs. AmCyanPH-1-treated samples in (c) (*$P < 0.05$, ***$P < 0.001$). Duncan's multiple range tests were used to compare the H_2O-treated samples (capital letters at $P < 0.05$) and the AmCyanPH-1-treated samples (small letters at $P < 0.05$) in (c). *Actin* was used as the internal control. Error bars are the standard error of the mean (SEM). Relative data of independent transgenic events refer to the main text (Fig. 5).

Fig. S13 *ICS* regulates floral resistance to Fusarium head blight (FHB) in T_2 transgenic barley. (a) AmCyanPH-1-based green fluorescence in infected florets of three barley lines labelled on the left. Each line was photographed in both bright field (top images of each set) and fluorescence (bottom images of each set). (b) Integrated fluorescence intensity (Integrated Fl. Int.) of the infected florets: at least 10 florets were analysed for each genotype using ImageJ. (c) The expression of *ICS* in infected florets. Tukey–Kramer's tests plus a pdiff option were used to compare transgenic vs. wild-type (WT) plants in (b), and Dunnett's tests were used to compare transgenic vs. WT plants in (c) (*$P < 0.05$, ***$P < 0.001$). *Actin* was used as the internal control. Error bars are the standard error of the mean (SEM). Relative data of independent transgenic events refer to the main text (Fig. 6). hai, hours after inoculation.

Table S1 Barley genes used in the current study.

Table S2 Genetic transformations of different target genes in barley.

Table S3 Transgene segregation in the T_1 generation.

Table S4 Plant height and tiller number of assayed transgenic events.

Table S5 Polymerase chain reaction (PCR) primers used in the current study.